



Production of iron nanoparticle by using *Aloe vera* gel and studying its effect on *Lepidium sativum* seed germination

Sundus Hameed Ahmed*, Rasha Saatam Hameed, Hassan Thamir, Hashim Kadhum Mohammed, Rana Al- Roomi, Isam Hussain T. Al-Karkhi

¹College of Science, Al- Mustansiriyah University, Baghdad, Iraq

²College of Dentistry, University of Baghdad, Iraq

Key words: UV, XRD, FTIR, *Aloe vera*, *Lepidium sativum*.

<http://dx.doi.org/10.12692/ijb/13.4.248-225>

Article published on October 22, 2018

Abstract

To synthesized and characterized green iron nanoparticles extracted from plants. Synthesis of iron bio-nanoparticles was done by using *Aloe vera gel* water extract as un-reducing agent. Characterization of Iron nanoparticles was performed using UV, XRD, and FTIR. The diameter of iron nanoparticles was about 52 nm. The effect of the exposure of *Aloe vera* seeds to iron nanoparticles on germination of *Lepidium sativum* has been studied. Seeds were exposed to green iron nanoparticles. Germination percentage and root shoot length were calculated. The results showed a reduction in germination percentage on exposure to 1000ppm of green nanoparticles while maximum germination percentage was on application of iron nanoparticles at 500ppm. Root and shoot growth was enhanced under iron nanoparticles application while reduction in root and shoot length was observed on exposure to 1000ppm of nanoparticles and Fe.

*Corresponding Author: Sundus Hameed Ahmed ✉ drsundusahmed@uomustansiriyah.edu.iq

Introduction

Synthesis Green iron nanoparticles, instead of using chemical reducing agent such as sodium borohydride which is flammable and corrosive (Khenfouch *et al.*, 2016). Now a day's researcher used extracts of plant part in preparing nano particles (Nyangiwe *et al.*, 2015).

These tiny products also have a large surface area to volume ratio, which is their most important feature responsible for the widespread use of nanomaterials in mechanics, optics, electronics, biotechnology, microbiology, environmental remediation, medicine, numerous engineering fields and material science (Sone *et al.*, 2017). Different protocols have been designed for the production of metallic nanoparticles. Chemical physical, electrical and Biological (Sundus *et al.*, 2013).

The coating is used to stabilize the particles in colloidal form, to prevent them from degradation and to minimize the toxicity. Generally, magnetite and maghemite are the two important forms of iron oxide, which are used as the magnetic materials for biomedical applications (Sundus *et al.*, 2017).

Agglomeration of magnetic nanoparticles is inevitable, because of their Vander Waals attractive forces between the tiny particles. Magnetite (Fe₃O₄) nanoparticles are chemically stable and non carcinogenic and has high saturation value (92emu/g) compared to the maghemite bulk material.

The production of iron nanomaterials, such as metallic iron and oxide of iron via a more convenient greener route, is a great step forward in the development of nanomaterials. This review highlights the significance of biogenic approaches and the role of biocompatible green materials in technological and economically feasible process and practices (Sundus 2018).

The main objective of the current study is to preparation green iron nano particles by using *Aloe vera* gel and characterize it by absorption

spectrophotometer (UV- VIS), X-ray diffraction (XRD), and scanning electron microscope (FTIR).

Studying Several indexes during the germination seed of *Lepidium sativum* such as root length, shoot length, fresh weight and germination ratio. To the best of our knowledge, it is the first reports focused on the effect of *Lepidium sativum* seeds germinating after exposing to *Aloe vera* iron nano particles nanoparticles with different morphologies.

Materials and methods

Plant material processing

The plant *Aloe vera* sample collected from home Garden. Fresh and healthy leaves were excised, washed with distilled water, then cut the leave to extracted the gel as shown in Figure 1.

Total Phenols

The total phenol compounds were detected by taking 150 µL of peel fruit crude extract (2 mg/ml D.W.) then reagent of Folin–Ciocalteu was added and mixed well for five minutes, then 2 ml of 20% sodium carbonate were added.

The mixture was put in the dark for 60 minutes. Absorbance was measured at 650 nm. Total phenols were quantified from calibration curve obtained by measuring the absorbance of known concentration of Gallic acid (Fuku *et al.*, 2016).

Detection of Flavonoids

The total flavonoids were measured according to (Boghossian *et al.*, 2013). Peel extract (0.1g) were added to 5 ml distilled water, then 5 ml ammonia solution was added, stirred well then mixed with 1 ml sulfuric acid. Yellow color refers flavonoids component.

Detection of alkaloids

Peel extract 0.5 g was added to 3 ml of hexane mixed well then 5 ml of 1% HCl, was added heating the mixture till boiling, 1-3 drops of picric acid were added. Yellow- colored precipitate appeared indicated alkaloids component.

Detection of terpenoids

Terpenoids content was determined as described by (Boghossian *et al.*, 2013). extract powder (0.5 g) was mixed with 10 ml 90% methanol then 2 ml of chloroform and 3 ml of sulphuric acid were added and mixed well. Reddish brown color indicates the presence of terpenoids.

Detection of tannins

Tannins were measured according to (Boghossian *et al.*, 2013) by adding (0.5 g) of peel extract to 10ml distilled water then 2% of FeCl₃. A blue-green color appeared indicated tannins.

Detection of proteins

Protein content was measured by an assay as described by (Boghossian *et al.*, 2013). Violet color appearance suggest the presence of amino acids and proteins.

Biosynthesis of iron nanoparticles

The procedure as established by (Bolik and Koop 1991). Twenty five grams of plant material was added to 200 mL of deionizer water and heated at 80°C for 1 h on a magnetic stirrer hotplate for the extraction of bioactive components.

Solid residues were removed by filtering the resultant solution three times using Whitman filter paper. To 100 mL of filtered solution (pH:5.7) adjusted to 10, 0.01 g of iron sulfate hepta hydrate was added as a precursor salt and heated at 85°C for 2 h.

The color of the solution changed from brownish dye to dark blue color. Reaction mixture was cooled and centrifuged at 10,000 rpm for 10 min to collect the precipitate assumed as IONPs. The obtained precipitate was washed three times with distilled water, dried and annealed at 500°C to obtain highly crystalline IONPs.

Annealing was performed to ensure full crystallization of the nanoparticles as well as decomposition of any extra compound from the natural extracts, not involved in the biosynthesis reaction.

*IONP Characterizations**X-Ray Diffraction (XRD)*

In order to obtain the structural information of iron nanoparticle by using X-Ray Diffraction (XRD):

Experimental Condition: X-ray Tube : Cu(1.54060 Å)
Voltage : 40.0 kV Current : 30.0 mA Scan Range : 20.0000 <-> 100.0000 deg Step Size : 0.0200 deg
Count Time : 0.12 sec Slit DS : 1.00 deg SS : 1.00 deg
RS : 0.30 mm.

The characteristic broad peak at 2θ of 45° indicates that the zero valent iron is predominantly present in the sample. The size of the particles was determined using the Scherrer equation (Buchaman *et al.*, 2000).

$$CS = K\lambda / \beta \cos \theta$$

Where CS is the crystallite size

Constant (K) = 0.94

β is the full width at half maximum (FWHM)

Full width at half maximum in radius (β) = FWHM x π/180

λ = 1.5406 x 10⁻¹⁰, Cos θ = Bragg angle.

FTIR spectroscopy

The spectra of Fourier transform infrared generated by the radiation of electromagnetic absorption in the frequency range 500 to 4000 cm⁻¹.

The absorption and intensity of different active functional group indicate geometry features of these groups. FTIR spectra were taken using Shimadzu model.

Germination assay

Seeds of *Lepidium sativum* were immersed in a 10% sodium hypochlorite solution for 10 min to ensure surface sterility, then, they were soaked in DI-water, nanoparticle suspensions for about 2 h after being rinsed three times with DI-water (Burklew *et al.*, 2012). Seeds were inserted into cork spots each spot filled with bit moss figure (2).

We used two concentration of IONPs in compare with iron and control without treatment. Then, seed

germination percentage was calculated, and seedling root and shoot length was also measured.

Statistical analysis

Each treatment was conducted with three replicates, and the results were presented as mean standard deviation.

The statistical analysis of experimental data utilized the Difference Least Significant (L.S.D.) Each of the

experimental values was compared to its corresponding control.

Results

Aloe vera leaf (leaf skin and gel) showed that almost all of the chemical constituents are present: different groups of active components such as phenolic compounds, flavonoids, Alkaloids, Terpenoids, Tannins, Proteins, carbohydrates, saponin, and steroids (Table 1).

Table 1. Active components in *Aloe vera*.

Test	
Total phenol	+++ ++
Alkaloids	++++
Terpenoids	++++
Tannin	++ ++
Protein	+++ +
Carbohydrates	++ ++
Steroids	+++
Saponin	++ ++

Table 2. Over all view of nanoparticles impact on germination percentage after five days.

Treatment	% germination	Shoot length	Root length
FeNP 1000PPM	96	5.25 ± 0.37b	3.6 ± 0.2b
FeNP2 500PPM	100	7.45 ± 0.47a	5.3 ± 1.3a
Control	95	3.85 ± 0.4c	2.18 ± 1.7c
Fe	80	2.9 ± 0.34c	0.53 ± 0.5bc

Significant differences ($p < 0.05$) between means were indicated by different letters.

While Figure 1 shows the *Aloe vera* gel and Figure 2 shows the Bitmoss Spot. In table 2, four different types of treatment were studied and the impact of nanoparticles on germination percentage were studied in detail (after five days) on shoot length and root length (all the significant differences ($p < 0.05$) between means were indicated by different letters, and results were recorded in Table 2.

The UV-Visible Spectrometer spectrum of the nano iron particle where recorded in Figure 3. The pattern of XRD for the synthesized nano particles is depicted in Figure (4), while Figure (5) represents the flowchart of the FTIR spectrum of the synthesized magnetite nanoparticles. In Figure 6 the germinated lipidium sativum for the four groups (INO 1000PPM, INO 500PPM, Fe and the control) were clearly shows the differences between them.



Fig. 1. *Aloe vera* gel.

Discussion

Table 1 shows flavonoids are secondary metabolites, ubiquitous in fruitiest of different groups of active components and vegetables, which protect cell from

degradation, stress, and act as signaling molecules. Phytoalexins, detoxifying agents, reduce toxic effects and stimulants (Page 1982; Rasha *et al.*, 2018).



Fig. 2. Bitmoss spot.

Recent research indicated that active components can be nutritionally helpful by triggering the production of natural enzymes that fight disease, such as cancers, heart disease, and age-related degenerative diseases (Madison *et al.*, 2002; Salim and Sundus 2014). The

changing of extract color from pale brown to black color indicated Synthesized Iron Oxide nanoparticles by the reduction of Fe^{+2} to Fe^0 ions, then precipitate was washed with water and ethanol and kept for air dry as shown in Figure 3.

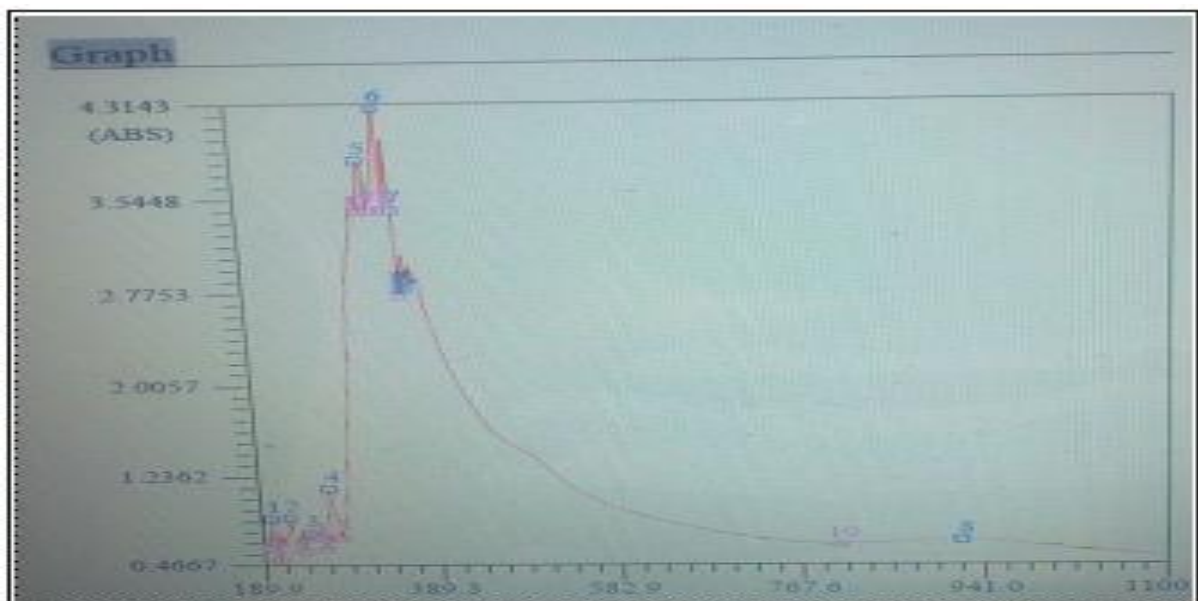


Fig. 3. UV- Visibel Iron Oxide nanoparticles.

The absorption of peak at wavelengths of 375nm indicates the formation of nano iron particles. The

pattern of XRD for synthesized as shown in Figure (4).

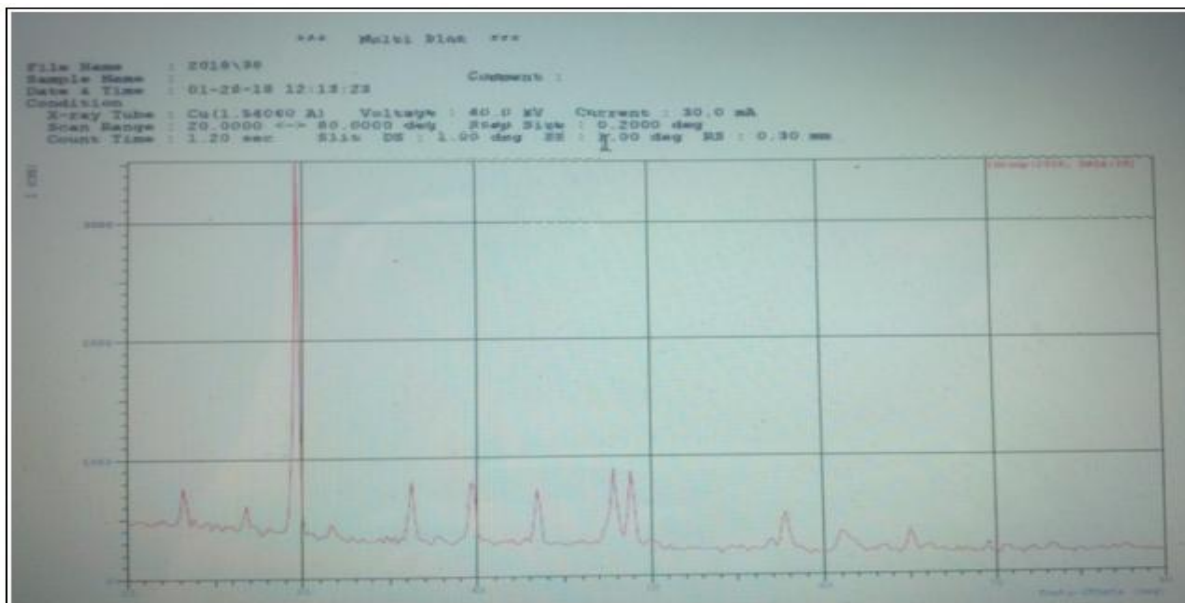


Fig. 4. XRD pattern of synthesized Iron nanoparticles.

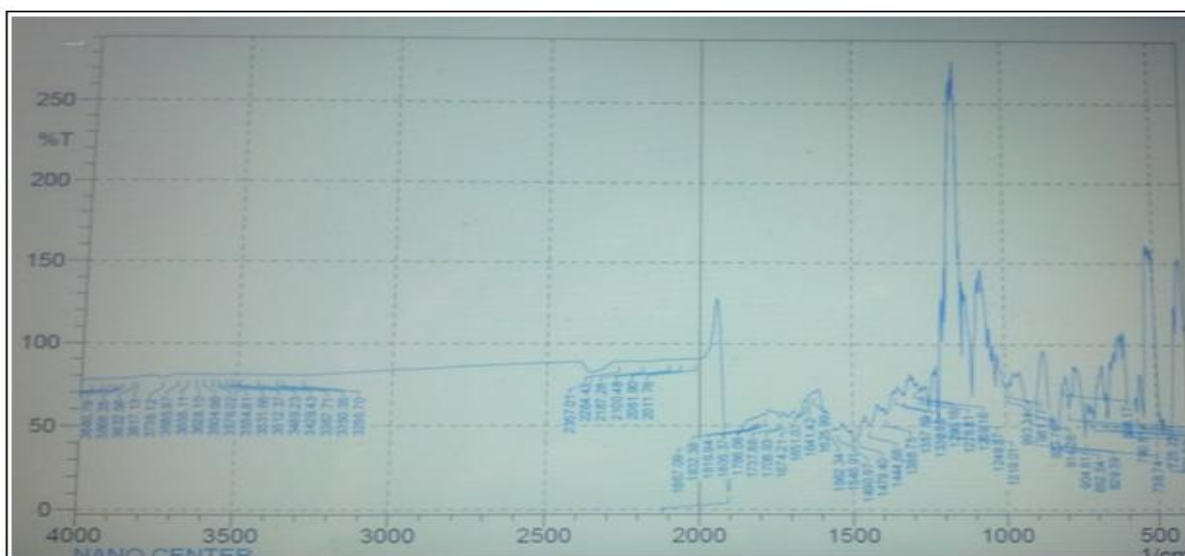


Fig. 5. FTIR spectrum of synthesized magnetite nanoparticles.

The intensity and position counts of the peaks diffraction of the sample were match with the standard XRD data for bulk magnetite (JCPDS No. 88-0866). The peaks which appeared at 38, 45, 65 and 78 can be assigned to the peaks of the Fe_3O_4 and particle size about 53 calculated by Scherrer equation. Figure (5) showed the spectrum of FTIR analysis, we found that the strong band absorption at 500 cm^{-1} assigned to Fe-O bond vibrations referred to the formation of Fe_3O_4 nanoparticles, it was reported

that the wave number 570 and 450 cm^{-1} referred to Fe_3O_4 (Donnini *et al.*, 2003).

The broad bands at 2000 cm^{-1} and 4000 cm^{-1} are assigned to O-H bending vibrations of water, on iron oxide nanoparticles surface was due to the phenolic compound in *Aloe* extracts while the absorption at 1300-1950 cm^{-1} referred to C-C stretching of aromatic rings in the synthesis of Fe_3O_4 nanoparticles (Donnini *et al.*, 2009).

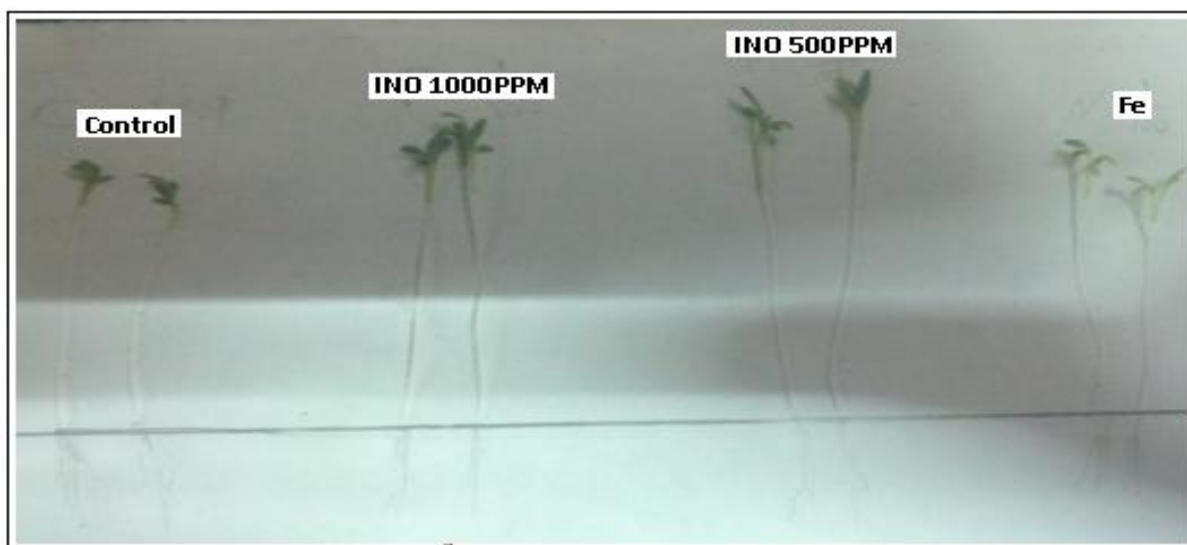


Fig. 6. Showed the germinated *Lepidium sativum*.

The absorption of peak at wavelengths of 425nm indicates the formation of nano iron particles.

Table 2 indicated that all four types of treatments affected the rate of germination, germination percentage, shoot length, root length.

NPs stimulated the growth of *Lepidium sativum* roots and shoots at almost all concentrations, especially at the low concentration (500mg/L), and the high concentration (1000mg/L), which accorded with previous reports (El-Temseh and Joner 2012), it seems that relative low concentration significantly promoted the growth of *Lepidium* shoots and roots in our experimental condition. These positive responses could be due to the amplified uptake of the water and nutrient by the treated seeds (Rasha *et al.*, 2018). The relative tiny diameter of NPs (about 52nm), which was susceptible to plant roots (Sundus 2018). While the treatment with Fe showed the lowest germination and the length of shoot and root in compare with the other treatments (Figure 6), may be due to the iron toxicity while the *Aloe vera* nano particles may be remove the toxicity of iron heavy metal.

References

Bremner JM. 1965. Total nitrogen. In: Methods of Soil Analysis Part 2, ed. C. A. Black, 1149-1178.

Boghossian AA, Sen F, Gibbons BM, Sen S, Faltermeier SM. 2013. Application of nanoparticle antioxidants to enable hyperstable chloroplasts for solar energy harvesting. *Advanced Energy Materials*, **3**, 881-893.

<https://doi.org/10.1002/aenm.201201014>

Bolik M, Koop HU. 1991. Identification of embryogenic microspores of barley (*Hordeum vulgare* L.) by individual selection and culture and their potential for transformation by microinjection, *Protoplasma* **162**, 61-68.

Buchanan BB, Grussem W, Jones RL. 2000. *Biochemistry and Molecular Biology of Plant*. Courler Companies, Inc., Maryland.

Burklew CE, Ashlock J, Winfrey WB, Zhang B. 2012. Effects of aluminum oxide nanoparticles on the growth, development and micro RNA expression of tobacco (*Nicotiana tabacum*). *PLOS ONE*, **7(5)**, e34783.

<http://dx.doi.org/10.1371/journal.pone.0034783>

Page AL. 1982. *Methods of Soil Analysis. Part 2*. Madison, WI: American Society Agronomy.

Donnini S, Castagna A, Guidi L, Zocchi G, Ranieri A. 2003. Leaf responses to reduced iron availability in two tomato genotypes: t3238 fer (iron

efficient) and t3238 fer (iron inefficient), Journal of Plant Nutrition. **26**, 2137-2148.

Donnini S, Castagna A., Ranieri A, Zocchi G. 2009. Differential responses in pear and quince genotypes induced by Fe deficiency and bicarbonate. Journal of Plant Physiology **166**, 1181-1193.

El-Temsah YS, Joner EJ. 2012. Impact of Fe and Ag nanoparticles on seed germination and differences in bioavailability during exposure in aqueous suspension and soil. Environmental Toxicology **27**, 42-49.

Fuku X, Kaviyarasu K, Matinise N, Maaza M. 2016. Punicalagin green functionalized Cu/Cu₂O/ZnO/CuO nanocomposite for potential electrochemical transducer and catalyst, Nanoscale Research letters **11(1)**, 386.
<http://dx.doi.org/10.1186/s11671-016-1581-8>

Khenfouch M, Minnis NR, Diallo A, Khamlich S, Hamzah M, Dhlamini M, Mothudi B, Baitoul M, Srinivasu V, Maaza M. 2016. Artemisia herba-alba Asso eco friendly reduced few-layered graphene oxide nanosheets: structural investigations and physical properties. Green Chemistry Letters Review **9(2)**, 122-131.
<https://doi.org/10.1080/17518253.2016.1181791>

Madison WI, Agron SCM, Cakmak I. 2002. Plant nutrition research: Priorities to meet human needs for food in sustainable ways. Progress in Plant Nutrition: Plenary Lectures of the XIV International Plant Nutrition Colloquium, The Netherlands. Caglar KO. 1949. Soil Science. Ankara, Turkey: Ankara University, Agricultural Faculty.

Nyangiwe NN, Khenfouch M, Thema F.T., Nukwa K, Kotsedi L, Maaza M. 2015. Free-green

synthesis and dynamics of reduced graphene sheets via sun light irradiation. Graphene **4(3)**, 54-61.
<http://dx.doi.org/10.4236/graphene.2015.43006>

Rasha SH, Rajwa HE, Sundus HA, Al-Karkhi IH. 2018. Study the Effect of Citrus aurantium Leaves Water Extracted Coper Nano Particles on the 3th, 4th Larave and Pupa of Culex pipiens, Pakistan Journal of Biotechnology **15(1)**, 101-106.

Salim Al-T, Sundus HA. 2014. Heavy Metals in Canned, Fresh and Frozen Fish from Local Iraqi Markets, International Journal for Sciences and Technology, **143(1733)**, 1-10.

Sone B, Diallo A, Fuku X, Gurib-Fakim A, Maaza M. 2017. Biosynthesized CuO nano-platelets: physical properties & enhanced thermal conductivity nanofluidics. Arabian Journal of Chemistry, in press.
<http://dx.doi.org/10.1016/j.arabj.2017.03.004>.

Sundus HA. 2018. Evaluation of antioxidant and anti-mutagenic activity of naturally fortified honey with Curcuma longa extract, International Journal of Medical Research & Health Sciences **7(5)**, 136-142.

Sundus HA, Rajwa HE, Mohammad M. 2017. Evaluation, Antioxidant, Antimitotic and Anticancer Activity of Iron Nanoparticles Prepared by Using Water Extract of Vitis vinifera L. Leaves, Journal of Advanced Laboratory Research in Biology **8(3)**, 67-73.

Sundus HA, Shatha S, Farah D, Raad T. 2013. Evaluation of biosynthesis of nanoparticles using medicinal plant extract of its anti oxidant and anti microbial activities, International Journal for Sciences and Technology **143(1731)**, 1-10.